



ADSORPTION AND ELECTROCHEMICAL STUDIES OF THIO ACETAMIDE INHIBITOR ON GAS PIPELINE METAL IN NATURAL SEA WATER ENVIRONMENT

Mathusudhan. M^{1*}, Deepa Rani P², Kavitha.C³

Article History: Received: 26.02.2023

Revised: 11.04.2023

Accepted: 27.05.2023

Abstract

The pipeline system in the oil and gasoline industry is the heart for transportation of crude and refined petroleum. However, non-stop exposure of the pipeline surfaces to impurities and assets of corrosion inclusive of sulfur and chromate is absolutely unavoidable. This inhibitor is act as good efficient character in these studies. Many inhibitors are the usage of in plenty of papers in many researchers together with green inhibitors and additionally artificial inhibitors to keep away from the metallic corrosion. This paper pursuits to dispose of the steel corrosion the use of the synthetic inhibitors. This inhibitor is act as good efficient character in these studies.

Keywords: Electro Chemical studies, Temperature studies ,thio acetamide inhibitor (TAA), SEM,EDAX.

^{1*}Research scholar (17212022031004), UG and Research Department of Chemistry, Aditanar College of Arts and Science, (Aff. To Manonmaniam Sundaranar University Tirunelveli) Thiruchendur-628215.

²UG and Research Department of Chemistry, Aditanar College of Arts and Science, Thiruchendur-628215.

³UG and Research Department of Chemistry, Aditanar College of Arts and Science, Thiruchendur-628215.

DOI: 10.31838/ecb/2023.12.s3.425

1. Introduction

In oil and gasoline industries, the corrosion issue has always been of great importance, with consequences similar results to those of natural disaster. Corrosion normally takes place in oil and gas pipelines. Since the pipelines play the function of transporting oil and gas from the well heads to the processing facilities, they are exposed to the continuous chance of corrosion, from the date of commissioning as much as decommissioning or abandonment. According to [1], the rough estimation of the aggregate every year value of corrosion is \$1.372 billion, that's the full of surface pipeline and facility costs (\$589 million), down-hole tubing costs (\$463 million), as well as capital expenses (\$320 million). Corrosion inhibitors are one of the mediums implemented to minimize corrosion in petroleum industries. For an optimum inhibition to be carried out, the inhibitors the inhibitors need to be introduced above a certain minimal concentration. There are lot of strategies, e.g., cathodic protection [2,3], organic coatings [4–6], and application of first-rate corrosion-resistant alloys [7], that may be carried out to fight against corrosion, but film-forming inhibitors are nevertheless recognized to be the unrivalled method of defense for mild steel in an acidic environment [8,9]. The film-forming inhibitors are used in industries to create a molecular layer proper at the floor of the metal and aliphatic tail as a second layer in hydrocarbon to prevent the water from contacting the steel surface and causing corrosion [10]. Recently, the upward thrust of the "green" chemistry concept in the fields of science, technology and engineering [11,12] is restraining the application of commercial corrosion inhibitors by using enforcing certain theories or ideas to reduce the contamination [13] from being discharged

into the surroundings as well as coming up with the eco-friendly chemicals [14–16]. As a movement to support this concept, the use of green-based corrosion inhibitors like plant extracts [17], chemical drugs [18], and ionic liquids [19,20] are being practiced. These green inhibitors are natural compounds that function via the adsorption on the surface of the metal to save you the prevalence of corrosion. Furthermore, fruit-based corrosion inhibitors are also one of the natural elements utilized due to their richness in vitamins, minerals, and phenolic compounds. However, the corrosion inhibitors adhere to certain factors like concentration, rate of dispersion, velocity, temperature, film persistency, pH, flow regime, and fluid composition, as well as the presence of instabilities able to perturbate the flow in minimizing corrosion. In This research work based on temperature studies and electro-chemical methods synthetic Inhibitor (TAA) Thio acetamide using natural seawater medium.

2. Materials and methods

2.1 Specimen preparation

Gas Pipeline specimen were mechanically pressed cut to form different coupons, each of dimension exactly 20cm² (5x2x2cm), polished with emery wheel of 80 and 120, and degreased with trichloroethylene, then washed with distilled water cleaned, dried and then stored in desiccator for the use of our present investigations.

2.2 Preparation of stock solution/ Inhibitor

1gm of specific synthetic inhibitor is weighed into a digital chemical balance and its dissolved into a specific solvent Dimethyl Sulfoxide (DMSO) then its made up to a 100ml (SMF) using natural sea water. From this solution in a different concentration from 0 to 1000 ppm using

natural sea water and used throughout the experiments.

2.3 Preparation of specimen for Electrochemical studies

Electrochemical measurements were conducted by conventional three – electrode system including of Oil pipeline as working electrode with an exposed area 1cm^2 , a platinum electrode as counter electrode and saturated calomel electrode (SCE) as reference electrode. Before

$$IE\% = \frac{I_{\text{Corr}}(\text{blank}) - I_{\text{Corr}}(\text{inh})}{I_{\text{Corr}}(\text{blank})} \quad (1)$$

Where $I_{\text{Corr}}(\text{blank})$ and $I_{\text{Corr}}(\text{inh})$ are the corrosion current density values of carbon steel in the absence and presence of inhibitors.

Electrochemical Impedance Spectroscopy was performed in range of frequency 1Hz to 100KHz with the AC signal of amplitude 5mV using CH660E electrochemical analyser . The charge transfer resistance obtained from the diameter of the semicircle of the Nyquist plot. The inhibition efficiency (IE%) derived from EIS was calculated using the following equation

$$IE\% = \frac{R_{\text{ct}}(\text{inh}) - R_{\text{ct}}(\text{blank})}{R_{\text{ct}}(\text{inh})} \quad (2)$$

where, $R_{\text{ct}}(\text{Inh})$ = charge transfer resistance with inhibitor.

$R_{\text{ct}}(\text{blank})$ = charge transfer resistance without inhibitor.

2.4 Adsorption studies

(a) Langmuir adsorption isotherm

The Langmuir adsorption isotherm can be expressed by the following Equation-4.10 is given below [38-40].

$$\log C/\theta = \log C - \log K \quad (6)$$

Where θ is the degree of surface coverage, C is the concentration of the inhibitor solution and K is the equilibrium constant of adsorption of inhibitor on the metal surface.

(b) TEMKIN ISOTHERM:

Temkin adsorption isotherm, the degree of surface coverage (θ) is related to the inhibitor concentration (c) according to equation – (7)

$$\text{Exp}(-2a\theta) = KC \quad (7)$$

Rearranging and taking logarithm of both sides of equation (7) gives equation – 8

$$\Theta = (-2.303 \log k/2a) - (2.303 \log C/2a) \quad (8)$$

(c) FLORRY-HUGGINS ISOTHERM:

Florry- Huggins adsorption isotherm can be expressed according to equation (9)

$$\text{Log}(\theta/C) = \log K + x \log(1-\theta) \quad (9)$$

(d) FRUMKIN ISOTHERM

Frumkin adsorption isotherm is given by equation (10)

$$\log \{ [C]^* (\theta/1-\theta) \} = 2.303 \log K + 2\alpha\theta \quad (10)$$

where k is the adsorption –desorption constant and α is the lateral interaction term describing the interaction in adsorbed layer plots of $\log \{ [C]^* (\theta/1-\theta) \}$ versus θ as presented were linear which shows that the applicability of Frumkin isotherm.

(e) FREUNDLICH ISOTHERM:

testing, the working electrode was immersed in test solution at Open Circuit Potential for 30 min to attain a steady state potential and the potential sweep rate for potentiodynamic polarization (Tafel) curves was 10mVs^{-1} . Corrosion current density (I_{Corr}) determined from the intercept of extrapolation of anodic and cathodic Tafel slopes at the corrosion potential (E_{Corr}). The inhibition efficiency (%) was calculated using I_{Corr} values both in the presence and absence of inhibitor.

The Freundlich adsorption isotherm can be also be applied using equation – (11)

$$\theta = Kc^n \text{-----(11)}$$

Freundlich model equation(6) can be rearranged as (12),

$$\log \theta = \log K + n \log C \text{-----(12)}$$

This will be drawn through $\log \theta$ vs $\log C$ from the intercept of the values k may be received. determined the values of the slopes and intercepts had been taken from the directly line equations.

(f) EL AWADY ISOTHERM:

The El-Awady adsorption isotherm is given by (13)

$$\log(\theta/1-\theta) = \log K + y \log C \text{-----(13)}$$

$k_{ads} = k_1/y$ and y represents occupying a given active site value of $1/y$ much less than cohesion implies the formation of multilayer of the inhibitor at the metal floor, while the value of $1/y$ extra than unity way that a given inhibitor occupy more than one active site.

2.5 Free Energy of Adsorption

The Equilibrium constant of adsorption of dimethyl sulfoxide extract of (TAA) on the surface of Gas Pipeline metal is related to the free energy of adsorption (ΔG) according to equation (14)

$$\Delta G = -2.303RT \log (55.5K) \text{-----(14)}$$

Where R is the gas constant, T is the temperature, K is the equilibrium constant of adsorption.

2.6 Activation Parameters on the Inhibition Process:

Usually, the temperature plays an important role to understanding the inhibitive mechanism of the corrosion process. To assess the temperature effect, experiments were performed at the range of temperature 303K- 333K in uninhibited and inhibited solutions containing different concentrations of TAA and the corrosion rate was evaluated and the values are presented in Table-3. The relationship b/w the corrosion rate (CR) of Gas Pipeline metal in natural sea water medium and temperature (T) is expressed by the Arrhenius equation (15)

$$\log CR = -E_a/2.303RT + \log \lambda \text{-----(15)}$$

Experimentally the values of corrosion rate evaluated from the weight loss data for Gas Pipeline metal in Natural Seawater in the presence and absence of TAA was used to determine the activation of enthalpy (ΔH) and apparent entropy (ΔS) for the formation of the complex in the transition state equation (16). An alternative formula for the Arrhenius equation is the transition state

$$CR = RT/Nh \exp(\Delta S/R) \exp(-\Delta H/RT) \text{-----(16)}$$

2.7 Corrosion products analysis

After the exposure tests, the surfaces of the exposed specimens were cleaned by an air blast to remove sea water content. The microstructure morphologies of the exposed surface of the samples were characterized by the Quanta 250 SEM-EDS system, and the corrosion products were analyzed by energy dispersive X-ray spectroscopy (EDS). Spot analysis was performed to understand the composition of

different features on the surface. The morphology of corrosion surface was also obtained after the corrosion products were removed.

2.8 NON- ELECTROCHEMICAL METHOD.

2.8.1. Effect of Temperature

Dissolution behavior of gas pipeline in natural seawater containing various concentration of Thio acetamide inhibitor

solution at temperature range from 303 to 333K and the observed values are listed in Table-1. These result reveals that the corrosion rate decreased with increase of inhibitor concentrations and also increased with rise in temperature from 303 to 333K. The maximum of 62.27% inhibition efficiency is achieved at 333K. However the effect of inhibition efficiency is increased with rise in temperature may suggests and support the facts that the

process of adsorption follows chemisorption. The obtained results suggests that the inhibitor may function through adsorption on the Gas pipeline metal surface by blocking the active sites to form a screen onto the metal surface from natural seawater. The percentage of inhibition efficiency increased with increase of inhibitor concentration and temperature.

Table-1 The corrosion parameters of gas-pipe line metal in Natural seawater containing various conc. of TAA inhibitor at different temp. after one hour exposure time.

Conc (ppm)	Weight loss (mg)			Corrosion rate (mmpy)			Inhibition efficiency (%)		
	303K	313K	333K	303K	313K	333K	303K	313K	333K
0	602	556	509	168.99	156.08	142.88	----	---	---
10	504	437	418	141.48	122.67	117.34	16.27	21.40	17.87
50	455	425	340	127.72	119.037	95.44	24.42	23.73	33.20
100	426	383	316	119.58	107.51	88.708	29.23	31.11	37.91
500	361	357	286	101.34	100.21	77.79	40.03	35.79	45.55
1000	299	254	192	83.936	71.303	53.89	50.33	54.31	62.27

2.8.2 Adsorption Studies.

The adsorption Process are very important surface phenomenon to determine the corrosion rate of reaction mechanism. The most frequently use of isotherms are viz: Langmuir, Temkin, Frumkin, Flory- Huggins, Freundlich, Parson's and the El-Awady, thermodynamic-kinetic model.

(a) Langmuir Isotherm:

Plotting $\log(C/\theta)$ against $\log C$ gave a linear relationship as shown in fig- 1.1(a), and the adsorption parameters are presented in Table-2. The average regression value ($R^2= 0.9976$) is very close to unity suggests that the adsorption of solution of TAA on surface of gas pipe line metal. The adsorptive interaction of TAA inhibitor was found to obey Langmuir isotherm.

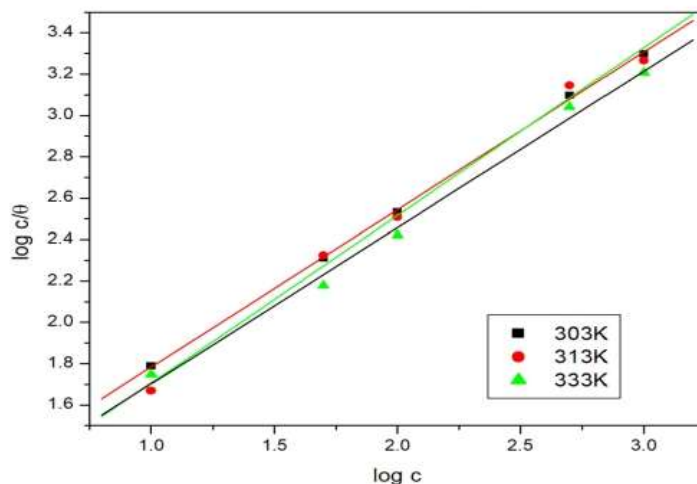


Fig-1.1(a) Langmuir isotherm for adsorption of dimethyl sulfoxide solution of (TAA) inhibitor on gas pipeline metal.

(b). Temkin Isotherm:

Plots of θ against $\log c$ are presented in fig-1.1(b) gave linear relationship, which shows that the adsorption data fitted with Temkin Adsorption Isotherm. Adsorption parameters were obtained from Temkin adsorption isotherm has been recorded in

Table-2. The average regression coefficient value is ($R^2 = 0.9511$). It's far away from the unity. However the attractive parameters (a) are positive values in all cases, because there is no repulsion exists in the adsorption layer.

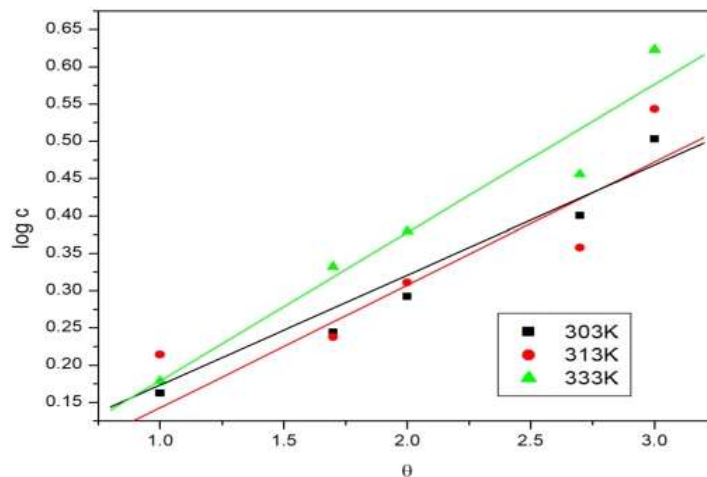


Fig- 1.1(b) Temkin isotherm for adsorption of dimethyl sulfoxide solution of (TAA) inhibitor on gas pipeline metal.

(c) Florry-Huggins Isotherm:

The plots of $\log \theta/c$ against $\log (1 - \theta)$ are shown in fig-1.1(c), and this data conformed to Florry huggins isotherm with average regression co-efficient (R^2) value is

0.9576. It is very far away from unity. The values of the size parameter 'x' are positive as shown in Table-2. This indicates that the adsorbed species of dimethyl sulfoxide solution of thioacetamide synthetic

inhibitor is bulky. Since the (Sulfur & Nitrogen) atoms are strongly adsorbed on the gas pipeline metal surface.

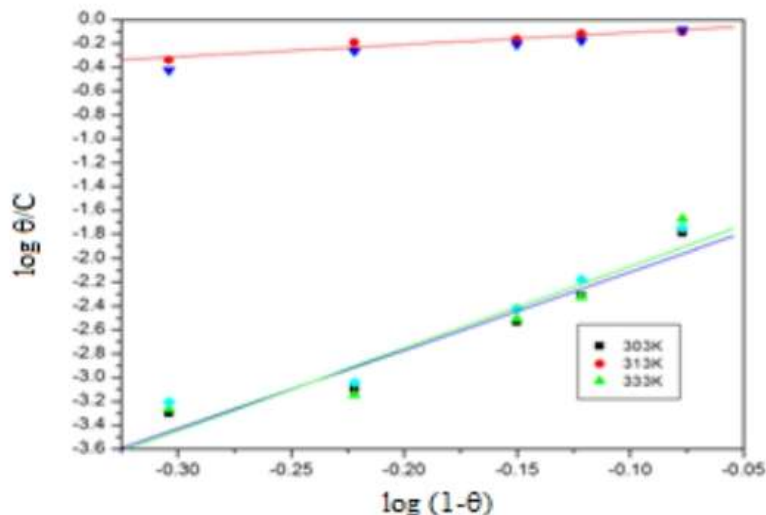


Fig-1.1(c). Florry-Huggins isotherm for adsorption of dimethyl sulfoxide solution of (TAA) inhibitor on gas pipeline metal .

(d) Frumkin Isotherm:

The values for Frumkin adsorption parameters were recorded in Table-2. Average regression co-efficient value ($R^2=0.9693$) is not close to unity. So this

inhibitor is didn't obey Frumkin adsorption isotherm. Also shows that values of the adsorption parameters ' α ' are positive suggest that the attractive behaviour of the inhibitor on the surface of Gas Pipeline metal.

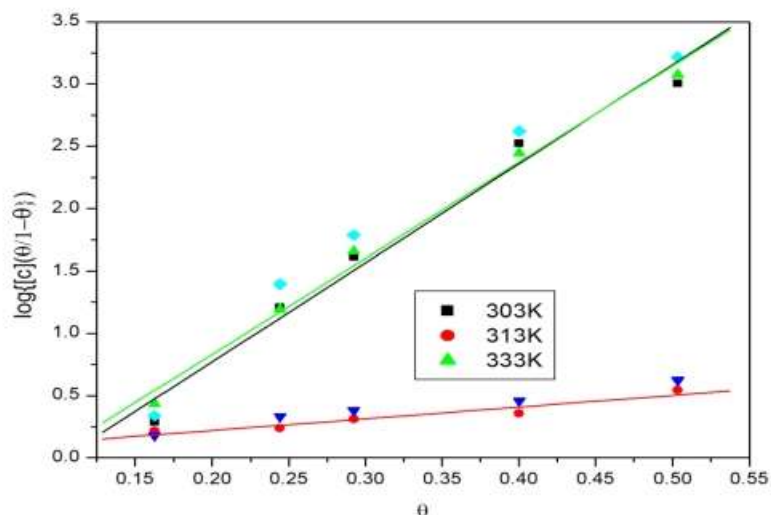


Fig-1.1(d) Frumkin isotherm for adsorption of dimethyl Sulfoxide Solution of (TAA) inhibitor on gas pipeline metal.

(e) Freundlich Isotherm:

The better values of suggests that the inhibitor is strongly adsorbed on the metallic floor. The value of the exponent 'n' gives an indication at the favourability of adsorption. It's far typically designated

that values of 'n' with the range 2-10 depict true, 1-2 reasonably tough and much less than 1 poor adsorption traits. For this reason Thio acetamide inhibitor (TAA) adsorbed on the metal floor by using bodily manner.

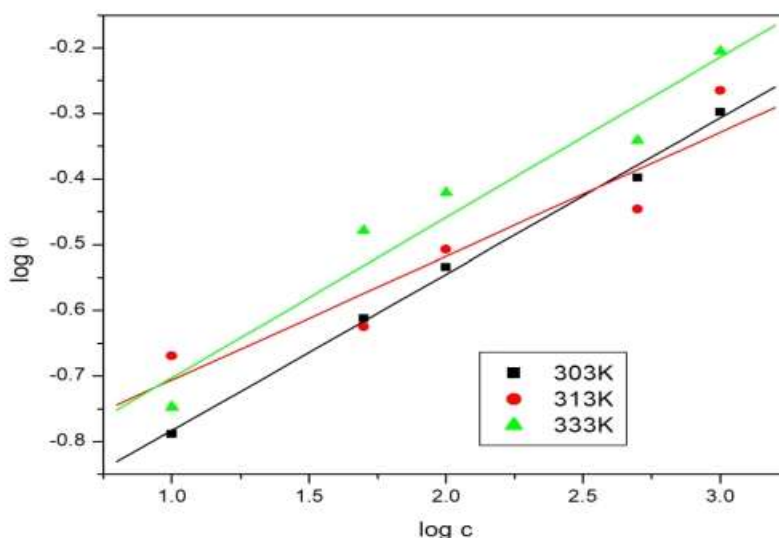


Fig-1.1(e). Freundlich isotherm for adsorption of dimethyl sulfoxide solution of (TAA) inhibitor on gas pipeline metal.

(f) El-Awady Isotherm:

The El-Awady adsorption isotherm is given by 4.17

$$\text{Log} (\theta/1-\theta) = \text{log K} + y\text{logC}$$

$k_{ads} = k_1/y$ and y represents occupying a given active site. Value of $1/y$ less than 1 implies that the inhibitor is formed in multi layer on the metal surface, while the value of $1/y$ greater than 1 means

that a given inhibitor may occupy more than one active site. Curve fitting of the data to the thermodynamic/kinetic model is shown in fig -1.1(f). Plot gives straight lines which show that the experimental data fits the isotherm. The values of k_{ads} and $1/y$ calculated from the El-Awady et.al, isotherm model is listed in Table -2

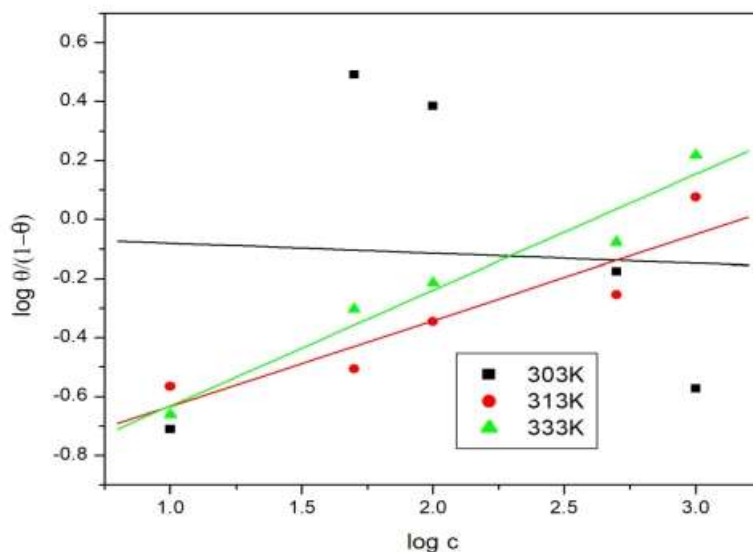


Fig-1.1 (f). El-Awady isotherm for adsorption of dimethyl sulfoxide solution of (TAA) inhibitor on gas pipeline metal.

(g) Free Energy of Adsorption:

The free energy of adsorption was calculated from values of ‘k’ obtained from Langmuir, Temkin, Florry –Huggins, Frumkin, Freundlich and El-Awady according to equation–9 and is observed in Table-2. This behaviour indicates the intensive interaction between the thioacetamide inhibitor and the metal

surface. As a common concept, the values of ΔG_{ads} up to -20 kJ mol^{-1} are associated with the electrostatic interaction of the charged compounds with the charged surface in which the adsorption process, in this case, is only physical. With increasing the values of ΔG_{ads} above -40 kJ mol^{-1} the chemical adsorption will be found.

Table-2. Adsorption parameters for adsorption of dimethyl sulfoxide solution of TAA on Gas Pipeline metal.

Isotherm	Temperature	R ²	K	ΔG_{ads} kJ/mol	Slope values
Langmuir	303K	0.9991	10.496	-16.041	-
	313K	0.9965	7.8469	-15.815	
	333K	0.9968	8.8509	-17.156	
Temkin	303K	0.9838	0.9511	-9.9925	a 0.0250
	313K	0.8983	1.0621	-10.610	0.0301
	333K	0.9710	0.9710	-10.996	0.2222
Florry-Huggins	303K	0.9659	0.0351	-1.6805	x 6.5802
	313K	0.9608	0.9873	-1.0420	1.0159
	333K	0.9460	0.0418	-2.3359	6.8843

Frumkin	303K	0.9879	0.1510	-5.3570	A 3.9760
	313K	0.9363	0.1979	-6.2381	3.7028
	333K	0.9836	0.1694	-6.1806	3.3566
Freundlich	303K	0.9979	0.0952	-4.1957	n 0.2379
	313K	0.9410	0.1274	-5.0916	0.1886
	333K	0.9711	0.1129	-5.0825	0.2443
El-Awady	303K	0.5409	0.1770	-5.7571	1/y 7.2992
	313K	0.9591	0.1437	-5.4041	4.3157
	333K	0.8508	0.1643	-6.1197	4.2498

2.8.3 Thermodynamic /Activation Parameters on the Inhibition Process.

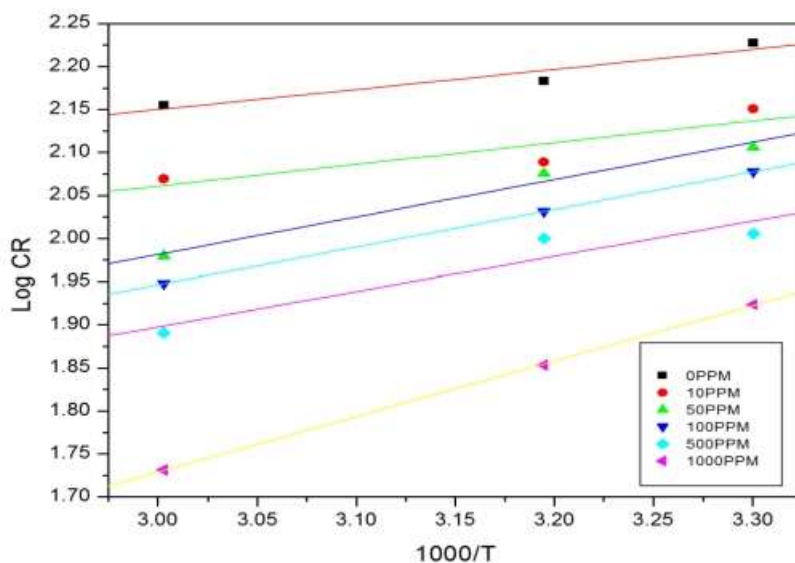


Fig-1.2 (g). Arrhenius Plot for Gas Pipeline metal corrosion natural Seawater in the presence and absence of different conc. of TAA inhibitor.

Plot of $\log(\text{CR})$ obtained by weight loss measurement versus $1/T$ gave straight line with common regression co-efficient (R^2) value far away from unity as shown fig-1.2(g). The values of apparent activation energy (E_a) obtained from the slope ($-E_a/2.303R$) of the lines and the pre-exponential factor (λ) obtained from the

intercept ($\log \lambda$) are given in Table-3. It is evident from the Table-3 that the apparent energy of activation is increased in the addition of TAA inhibitor comparison to the uninhibited solution. These values ranged from 4.5903 to 12.3606 kJ/mol and lower than the threshold value of 80kJ/mol required for chemical adsorption. This

indicates that the adsorption of dimethyl sulfoxide solution of TAA inhibitor on Gas Pipeline metallic floor surface is Physical adsorption. Increase in the activation energy is attributed to appreciable increase in the adsorption of inhibitor on Gas

Pipeline metal surface by increase in the temperature. The increase in adsorption leads to lower in corrosion rate due to the lesser exposed surface area of the gas Pipeline metal towards natural seawater.

Table-3. Activation parameters of TAA in Natural Seawater.

Inhibitor conc. (ppm)	E_a (kJ/mol)	λ (mg/cm)	$-\Delta H$ (kJ/mol)	$-\Delta S$ (J/mol/k)
Blank	4.5903	27.100	3.1424	67.9838
10	4.8269	20.160	3.2450	68.008
50	8.3194	4.7648	4.7494	62.8362
100	8.3510	4.3461	4.7750	62.4662
500	7.8183	4.7065	4.5479	62.743
1000	12.3606	1.6132	6.5148	55.435

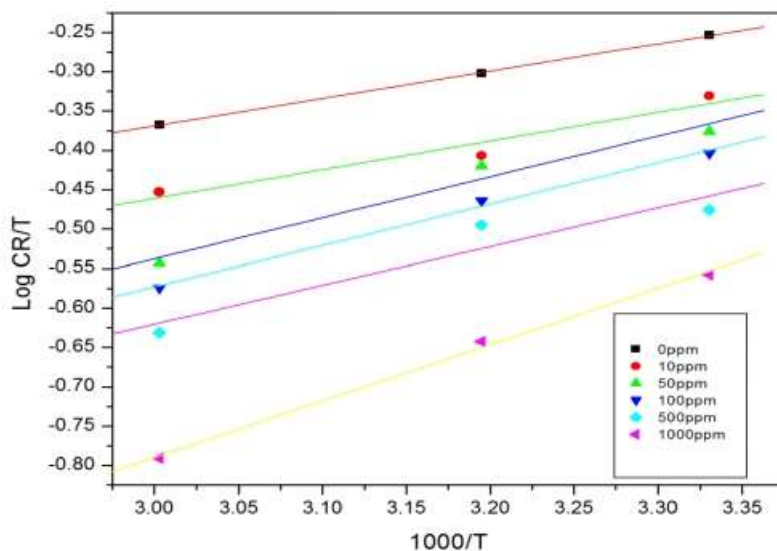


Fig-1.3 (h). Transition state plot for Gas Pipeline metal corrosion in Natural Seawater in the presence and absence of different conc. of TAA inhibitor.

The value of λ is also lower for inhibited solution compared to the uninhibited solution. It is clear from equation (1) that corrosion rate is influenced by both E_a and λ . Moreover

increase in concentration of (TAA) inhibitor in leads to an Increase in the value of E_a , indicating that the weak adsorption of the inhibitor molecules on the metal surface.

A plot of $\log (CR/T)$ versus $1/T$ is shown in fig-1.3(h), a straight lines were obtained with slope $(-\Delta H/2.303R)$ and intercept of $[\log(R/Nh)+ (\Delta S/2.303R)]$, from which ΔH and ΔS were calculated and listed out in Table-3. The negative value of enthalpy of activation (ΔH) in the presence and absence of various concentration of inhibitor reflects that the exothermic nature of Gas Pipeline metal. The values of entropy of activation (ΔS) listed in Table-3. It is clear that the entropy of activation decreased in the presence of the using inhibitor while as compared to free natural seawater. The decrease in the entropy of activation (ΔS) in the presence of inhibitor may decreased in the disordering on going from reactant to activated complex is difficult.

2.9. ELECTROCHEMICAL STUDIES

2.9.1. Polarization studies

The synthetic inhibitor in generally, have a promising corrosion inhibition tendency due to their capacity for the adsorptive contact with the surface,

which forms protective layers against corrosive media. Potentiodynamic polarization curves of Gas Pipeline metal immersed in natural seawater environment in the presence and absence of inhibitor are shown in fig-1.4. The corrosion parameters viz, corrosion potential (E_{CORR}), Corrosion current density (I_{CORR}), cathodic Tafel slope (b_c), and anodic Tafel slope (b_a) and percentage of inhibition efficiency (%IE) are given Table-4. E_{CORR} values shifted to negative potential with increase in concentrations of Thio acetamide solution. The corrosion current densities reduced from 74.02 to 27.95 μA with increase in concentrations of the inhibitor. According to the results of the test, b_c is somewhat greater than b_a , suggesting that the inhibitors favor cathodic rather than anodic action. As a result, these inhibitors function like a combination of inhibitors. Also, E_{corr} change slightly (less than ± 85 mV) which confirm that these compounds exert on both cathodic (hydrogen reduction) and anodic (metal dissolution) processes. So this inhibitor is mixed type.

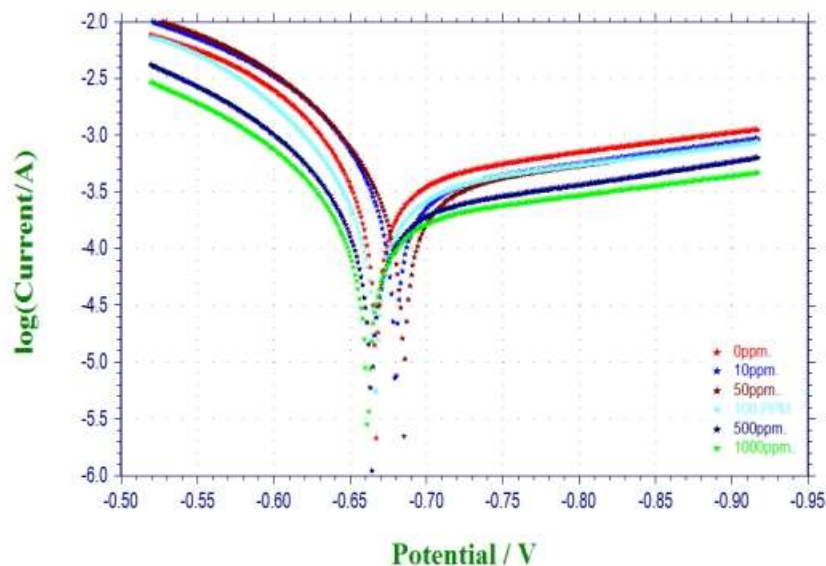


Fig-1.4 Polarization curves for Gas Pipeline metal in natural Seawater in the presence and absence of different conc. of TAA inhibitor.

Table-4 Parameters derived from electrochemical measurements of Gas Pipeline metal in natural seawater containing various conc. of TAA inhibitor.

Conc. (ppm)	Polarisation studies					Impedance studies		
	E_{corr} mV	b_a (mV/dec)	$-b_c$ (mV/dec)	I_{corr} μAcm^{-2}	I.E (%)	R_{ct} (Ω cm^2)	$C_{dl} \times 10^{-4}$ Fcm^2	I.E (%)
Blank	-667	2307	7288	74.02	---	9.743	0.00143	---
10	-679	2120	7767	68.3	7.72	9.830	0.00133	0.91
50	-685	2148	8832	53.2	28.12	10.499	0.00017	7.20
100	-667	2243	9218	41.99	43.27	12.288	0.0008	20.27
500	-664	2177	8421	31.41	57.56	13.396	0.0008	27.26
1000	-661	2019	7906	27.95	62.23	25.064	0.0002	61.27

2.9.2. Electrochemical impedance (EIS) studies

Fig-1.4 shows that typical set of complex planes plot of gas pipeline metal in natural seawater in the Presence and absence of various concentration of TAA inhibitor at room temperature. It was obvious that the addition of inhibitor results in an increase of the diameter is imperfect capacitive loops (Fig-1.5(a)), bode impedance plot (Fig-1.5(b)) and the maximum phase angle (Fig-1.5(c)). Careful inspection of this data revealed that the value of charge transfer resistance (R_{ct}) increased from 9.74 to 25.064 Ωcm^2 of gas pipeline metal natural seawater medium with increase of inhibitor concentrations. The inhibition efficiency increased from 0.91 to 61.27% with increase of inhibitor concentration. It ensures that the formation of protective film mask on the metal surface. The double layer capacitance (C_{dl}) decreased as the increase of inhibitor

concentration may be due to the adsorption of the active compounds on the metal surface leading to a film formation. It is able to be noticed that the dotted lines clearly indicated that the charge transfer process may controlling the dissolution of the metal. The Bode impedance plots (Fig-1.5(b)) reflected that the value of charge transfer resistance (R_{ct}) increased with increase of inhibitor concentration and suggested that the protective film formed on the metal surface was more stable. Since it was able to withstand the attack of aggressive corrosive environment. In Bode phase plots (Fig-1.5(c)) the phase angle at higher frequencies attributed to anticorrosion performance. The depression of phase angle at relaxation frequency with the decrease in the inhibitor concentration indicates that the decrease of capacitive response with the decrease of inhibitor concentration. Such a phenomenon

reflected that the higher corrosion activity at low concentrations of the inhibitor.

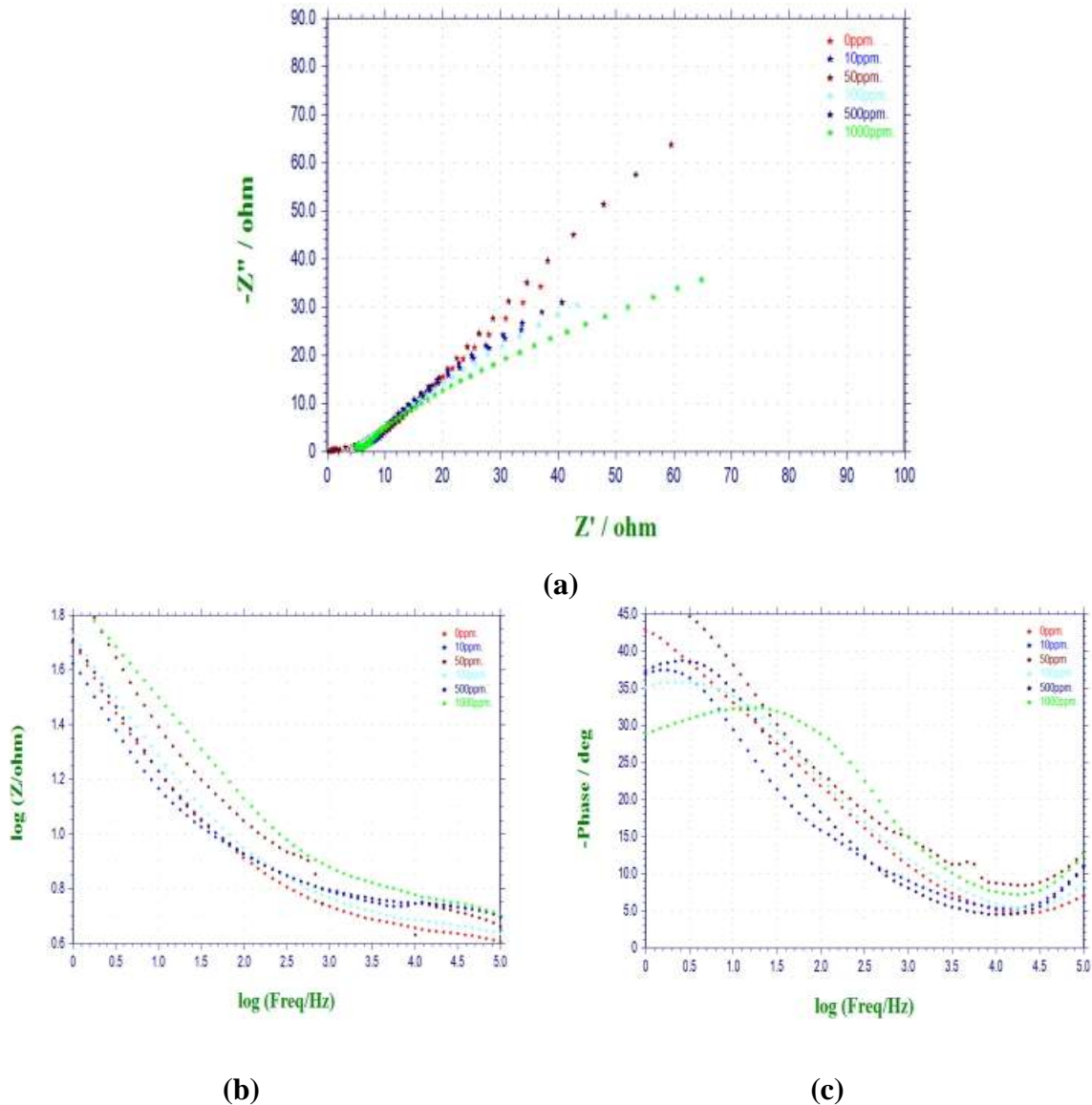


Fig-1.5(a-c). Electrochemical impedance plots, (a) Nyquist (b) Bode impedance plot (c) phase angle plot for Gas Pipeline metal in natural seawater containing various conc. of TAA inhibitor.

3.1 CHARACTERIZATION OF CORROSION COMPOSITES

3.1.1 EDAX Analysis

EDAX spectroscopy was used to predict the elements present on the Gas pipeline metal surface in the presence and absence of inhibitor. Fig-1.8 (a) and (b) reflects the EDAX spectra for the corrosion product on metal surface in the absence and presence of optimum concentrations of

TAA inhibitor solution in Natural seawater medium. In the absence of inhibitor molecules, the spectrum may be confirmed that percentage level of the atoms for iron (47.72%), Sulfur (0.29%) Sodium (0.14%). However in the presence of the optimum concentrations of the inhibitor. The percentage level the atoms in Sodium (0.22%), iron (43.79%), and sulfur (0.49%). It obviously indicates that the

hetero atoms present in the inhibitor molecules may be involved in complex formation with metal ions during the

adsorption process and to prevent the further dissolution of metal against corrosion.

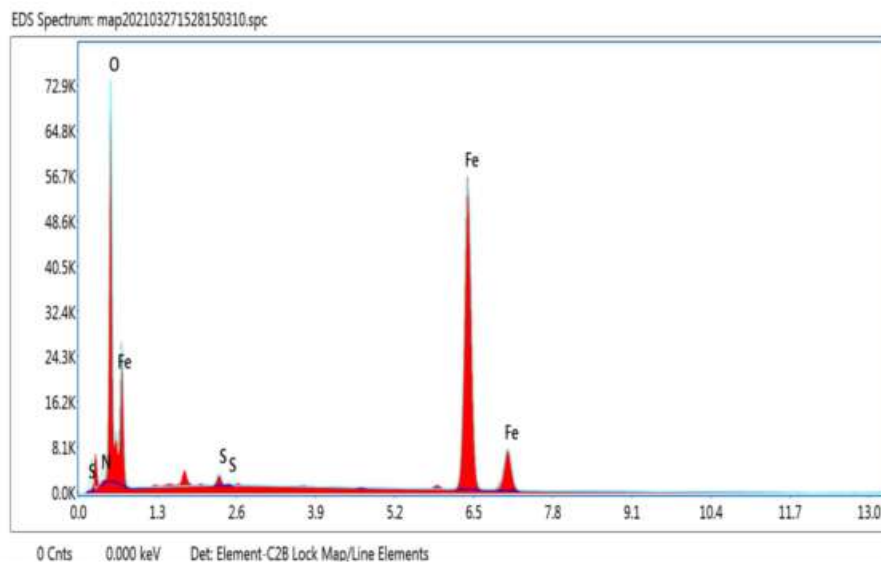


Fig-1.6.(a) EDAX spectrum of the corrosion product on Gas Pipeline metal in natural seawater alone.

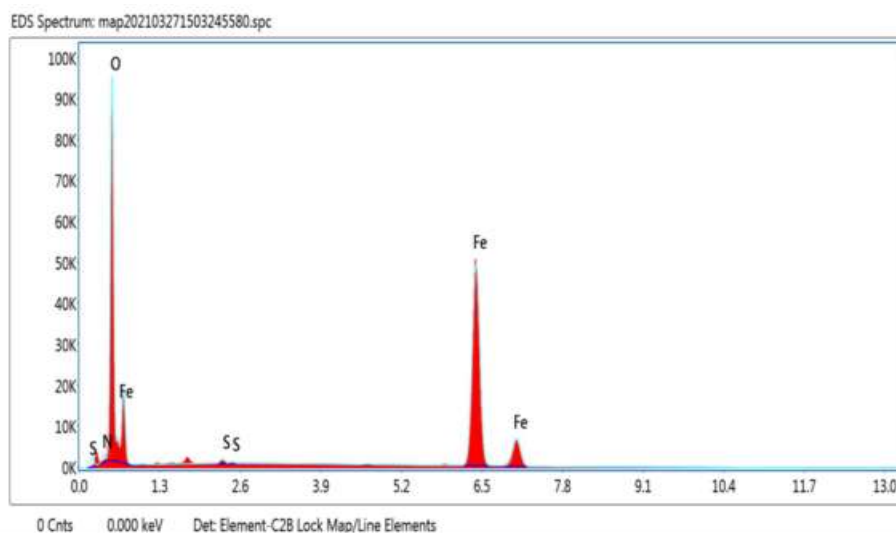
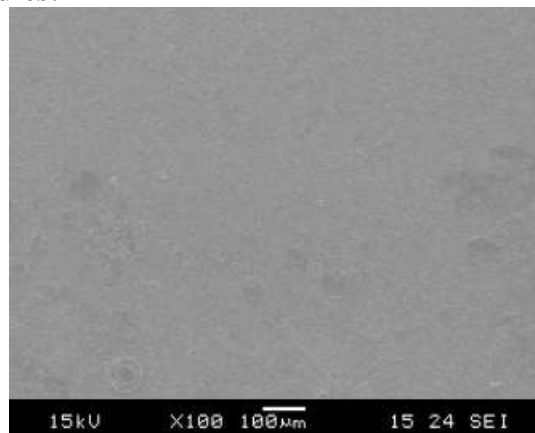
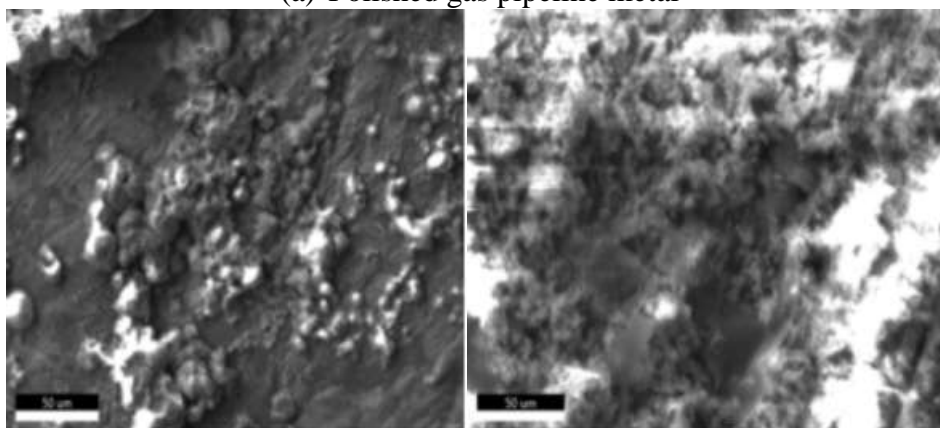


Fig-1.6.(b) EDAX spectrum of the corrosion product on Gas Pipeline metal in natural seawater with presence of inhibitor(TAA).

3.1.2 Morphological studies:



(a) Polished gas pipeline metal



b) Absence of inhibitor

(c) Presence of inhibitor

Fig-1.7 (a-c). SEM magnification of API-5L-Grade-X65 Gas Pipeline in natural seawater containing presence and absence of TAA inhibitor.

3.1.3 SEM Analysis.

Fig:1.7 (a-c) shows that the surface morphological view of Polished gas pipeline metal in compared the absence and presence of TAA inhibitor solution in natural seawater. The SEM image shows (a) The first one is Polished gas Pipeline metal. (b)The second image is rough

surface has occurred in the absence of inhibitor. (c)The third image is addition of TAA inhibitor was accompanied by the formation of a protective film, which can be explained by the adhesion of the inhibitor to the surface of the gas Pipeline metal, which suppresses the corrosion process.

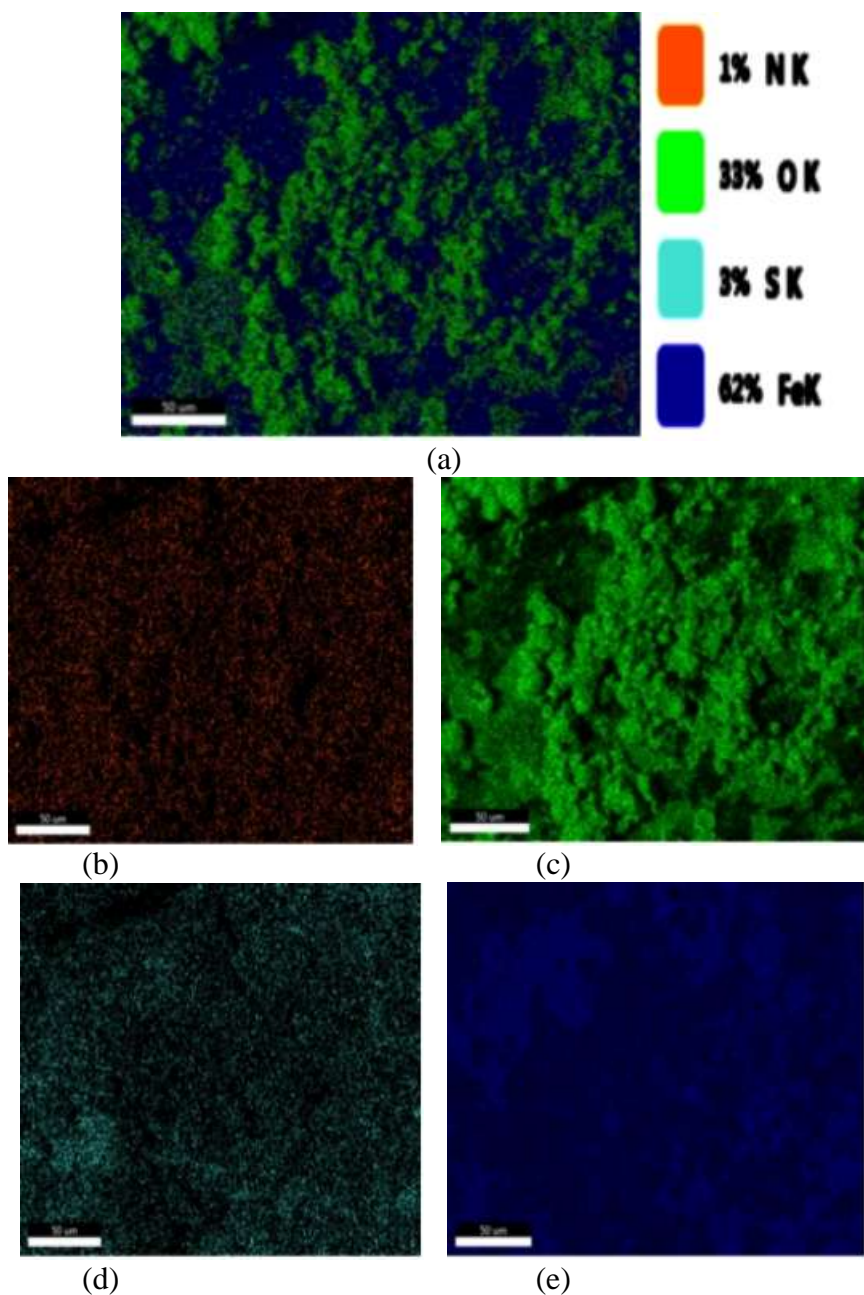


Fig-1.8(a) (a-e). These images shows the various percentage level atoms present in the elemental mapping in the absence of inhibitor. (a) Common mapping, (b) Percentage level of Nitrogen. (c) Percentage level of Oxygen. (d) Percentage level of Sulfur. (e) Percentage level of iron.

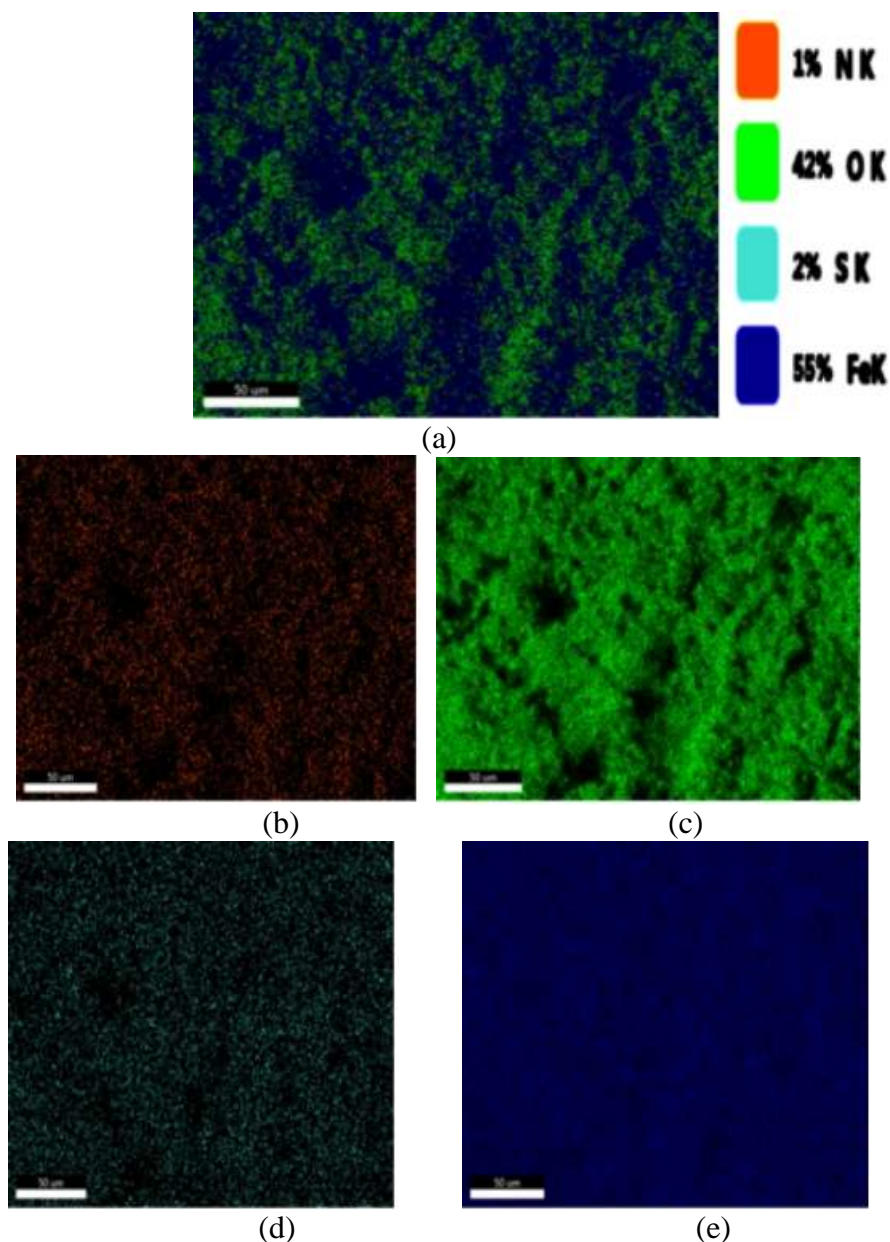


Fig-1.8(b) (a-e). These images shows the various percentage level atoms present in the elemental mapping in the Presence of inhibitor. (a) Common mapping, (b) Percentage level of Nitrogen. (c) Percentage level of Oxygen. (d) Percentage level of Sulfur. (e) Percentage level of iron.

3. CONCLUSIONS

Dissolution behaviour of Gas Pipeline metal was increased with the increase of exposure time and decreased with the increase of TAA inhibitor concentration. Maximum of 61.27% of inhibition efficiency was achieved at 1000ppm of TAA inhibitor

concentration. In temperature studies, the maximum of 50.33%, 62.27% was attained at 303K and 333K respectively. Values of E_a indicates that the adsorption of TAA inhibitor follows the mechanism of Physical adsorption. Inhibitor obeyed Langmuir ($R^2=0.9976$) adsorption isotherm and behave as mixed type. Thermodynamic parameters such as ΔH_{ads} and ΔG_{ads}

represented that the adsorption of TAA inhibitor solution on metal surface was exothermic and spontaneous process. In polarization studies the value of I_{corr} decreased from 74.02 to 27.95 μA and the maximum of 62.23% I.E was arrived in the presence of inhibitor. The R_{ct} values increased from 9.74 to 25.064 Ωcm^2 with increase of inhibitor concentration and the maximum of 61.27% of I.E was attained. EDAX spectral analysis may also confirm the formation of complex on the metal surface. The SEM image shows (a)The first one is Polished gas Pipeline metal. (b)The second image is rough surface has occurred in the absence of inhibitor. (c)The third image is addition of TAA was accompanied by the formation of a protective film, which can be explained by the adhesion of the inhibitor to the surface of the gas Pipeline metal, which suppresses the corrosion process.

4. REFERENCES

- Simon, M.R. Report of O_shore Technology Conference (OTC) Presentation; NACE International Oil and Gas production: Houston, TX, USA, 2008.
- Chen, R.; Li, X.; Du, C.; Cheng, Y. Effect of cathodic protection on corrosion of pipeline steel under disbonded coating. *Corros. Sci.* **2009**, 51, 2242–2245. [[CrossRef](#)]
- Yabuki, A.; Tanabe, S.; Fathona, I. Comparative studies of two benzaldehyde thiosemicarbazone derivatives as corrosion inhibitors for mild steel in 1.0 M HCl. *Surf. Coat. Technol.* **2018**, 341, 71–77. [[CrossRef](#)]
- Lyon, S.; Bingham, R.; Mills, D. Corrosion Protection of Carbon Steel by Pongamia glabra Oil- Based Polyetheramide Coatings. *Prog. Org. Coat.* **2017**, 102, 2–7. [[CrossRef](#)]
- Chengduan, W.; Chuan, L.; Bin, X.; Xiaogang, G.; Dong, F.; Bin, L. Corrosion inhibition of mild steel in HCl medium by S-benzyl-O,O-bis(2-naphthyl)dithiophosphate with ultra-long lifespan. *Results Phys.* **2018**, 10, 558–567.
- Salman, T.; Al-Azawi, K.; Mohammed, I.; Al-Baghdadi, S.; Al-Amiery, A.; Gaaz, T. Experimental and quantum chemical simulations on the corrosion inhibition of mild steel by 3-((5-(3,5-dinitrophenyl)-1,3,4-thiadiazol-2-yl)imino)indolin-2-one. *Results Phys.* **2018**, 10, 291–296. [[CrossRef](#)]
- Odeunmi, N.; Umoren, S.; Gasem, Z.; Ganiyu, S.; Muhammad, Q. Electrochemical and quantum chemical studies on carbon steel corrosion protection in 1M₂SO₄ using new eco-friendly Schi_ base metal complexes. *J. Taiwan Inst. Chem. Eng.* **2015**, 51, 177–185. [[CrossRef](#)]
- Zeino, A.; Abdulazeez, I.; Khaled, M.; Jawich, M.; Obot, I. Electrochemical Corrosion Performance of Aromatic Functionalized Imidazole Inhibitor Under Hydrodynamic Conditions on API X65 Carbon Steel in 1 M HCl Solution. *J. Mol. Liq.* **2018**, 250, 50–62. [[CrossRef](#)]
- Umoren, S.; Eduok, U. Application of carbohydrate polymers as corrosion inhibitors for metal substrates in different media: A review. *Carbohydr. Polym.* **2016**, 140, 314–341. [[CrossRef](#)]
- Yadav, D.; Maiti, B.; Quraishi, M. Electrochemical and quantum chemical studies of 3,4-dihydropyrimidin-2(1H)-ones as corrosion inhibitors for mild steel in hydrochloric acid solution. *Corros. Sci.* **2010**, 52, 3586–3598. [[CrossRef](#)]
- Hu, K.; Zhuang, J.; Zheng, C.; Ma, Z.; Yan, L.; Gu, H.; Zeng, X.; Ding, J. Effect of novel cytosine-l-alanine derivative

- based corrosion inhibitor on steel surface in acidic solution. *J. Mol. Liq.* **2016**, 222, 109–117. [[CrossRef](#)]
- Ramezanzadeh, B.; Vakili, H.; Amini, R. The effects of addition of poly (vinyl) alcohol (PVA) as a green corrosion inhibitor to the phosphate conversion coating on the anticorrosion and adhesion properties of the epoxy coating on the steel substrate. *Appl. Surf. Sci.* **2015**, 327, 174–181. [[CrossRef](#)]
- Mohammadinejad, R.; Karimi, S.; Iravani, S.; Varma, R. Plant-derived nanostructures: Types and applications. *Green Chem.* **2016**, 18, 20–52. [[CrossRef](#)]
- Varma, R. Journey on greener pathways: From the use of alternate energy inputs and benign reaction media to sustainable applications of nano-catalysts in synthesis and environmental remediation. *Green Chem.* **2014**, 16, 2027–2041. [[CrossRef](#)]
- Jeon, H.; Lim, C.; Lee, M.; Kim, S. Chemical assay-guided natural product isolation via solid-supported chemodosimetric fluorescent probe. *Chem. Sci.* **2015**, 6, 2806–2811. [[CrossRef](#)] [[PubMed](#)]
- Srivastava, M.; Tiwari, P.; Srivastava, S.; Prakash, R.; Ji, G. Electrochemical investigation of Irbesartan drug molecules as an inhibitor of mild steel corrosion in 1 M HCl and 0.5 M H₂SO₄ solutions. *J. Mol. Liq.* **2017**, 236, 184–197. [[CrossRef](#)]
- Mo, S.; Li, L.; Luo, H.; Li, N. An example of green copper corrosion inhibitors derived from flavor and medicine: Vanillin and isoniazid. *J. Mol. Liq.* **2017**, 242, 822–830. [[CrossRef](#)]
- Diamanti, M.; Velardi, U.; Brenna, A.; Mele, A.; Pedferri, M.; Ormellese, M. Compatibility of imidazolium-based ionic liquids for CO₂ capture with steel alloys: A corrosion perspective. *Electrochim. Acta* **2016**, 192, 414–421. [[CrossRef](#)]
- Lozano, I.; Mazario, E.; Olivares-Xometl, C.; Likhanova, N.; Herrasti, P. Corrosion behaviour of API 5LX52 steel in HCl and H₂SO₄ media in the presence of 1, 3 dibencilimidazolium acetate and 1,3-dibencilimidazoliododecanoate ionic liquids as inhibitors. *Mater. Chem. Phys.* **2014**, 147, 191–197. [[CrossRef](#)]
- El-Hajjaji, F.; Messali, M.; Aljuhani, A.; Aouad, M.; Hammouti, B.; Belghiti, M.; Chauhan, D.; Quraishi, M. Pyridinium-based ionic liquids as novel and green corrosion inhibitors of carbon steel in acid medium: Electrochemical and molecular dynamics simulation studies. *J. Mol. Liq.* **2018**, 249, 997–1008. [[CrossRef](#)]